Simulation of the dynamic aperture of the NICA booster synchrotron based on magnetic measurement data

Shandov M. M.[a], Kostromin S. A.[a, b]

[a] VBLHEP, Joint Institute for Nuclear Research, Dubna, Russia
[a, b] Saint-Petersburg State University, St. Petersburg, Russia

June 10, 2022

Topics

Introduction

Introduction

NICA Booster is a new superconducting synchrotron with operating energies up to 578 MeV/u. The first commissioning Run was successfully carried out in December 2020.

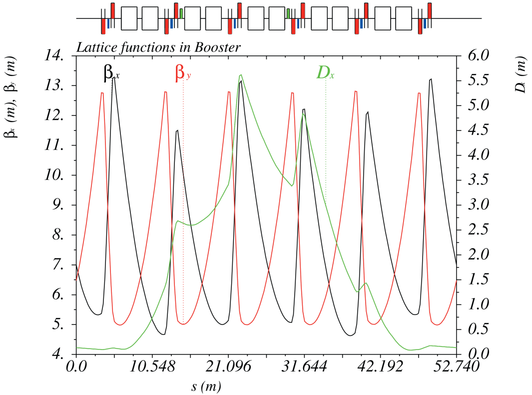

6 DFO-cells x 4 Superperiods

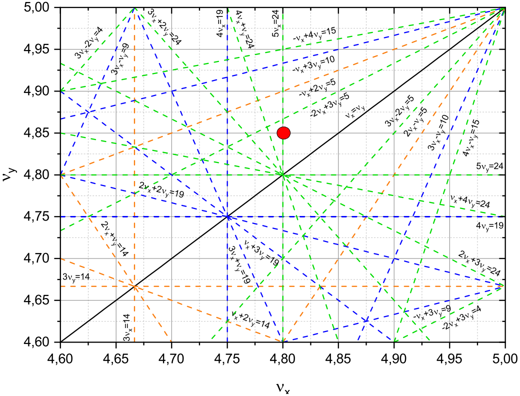

Woprking poing: $\nu_x/\nu_y = 4{,}8/4{,}85$

Introduction

Parameter	Value
Ion $^{197}_{31}Au$ energy, MeV/u	$3{,}2 \div 578$
Betatron tunes ν_x/ν_y	$4{,}80/4{,}85$
Natural chromaticity ξ_x/ξ_y	$-5{,}10/-5{,}50$
Ring acceptance, $\pi \cdot mm \cdot mrad$:	
horizontal	$305/150$
vertical	$80/58$
Beam emittance, $\pi \cdot mm \cdot mrad$:	
at the injection $\varepsilon_x/\varepsilon_y$	$15 \div 150/15$
at the end of acceleration $\varepsilon_x/\varepsilon_y$	$0{,}2 \div 3/0{,}2 \div 1{,}5$
Number of ions in the bunch	$3 \cdot 10^9$
Momentum spread $\Delta p/p$:	
at the injection	$\pm 10^{-3}$
maximal	$\pm 2{,}3 \cdot 10^{-3}$
at the end of acceleration	$\pm 5 \cdot 10^{-4}$
Revolution time, μs:	
at the injection	$8{,}51$
at the end of acceleration	$0{,}89$

Introduction

Dynamic aperture (or ***acceptance***) **(DA)** – domain of the particles are located (coordinates) in 6D phase space, where their motion in electromagnetic field of the facility is stable under the influence perturbations. Here the perturbations are:

- systematic and random errors of the lattice magnets and RF-stations;
- space charge force;
- impedance of the beam pipe;
- etc.

In this works, only **transvers** DA are considered (without the synchrotron motion).

Let us introduce the concept of the maximal initial amplitude of a particle oscillation:

$$A_{x,y}(s) \Leftrightarrow (x, x', y, y') : \forall N_{turn}, \exists A_{x,y}(s) > A'_{x,y}(s), N_{turn} \in \mathbb{Z}^{+}$$

$A'_{x,y}(s)$ – the geometrical acceptance of the facility.

Introduction

Dynamic aperture (or ***acceptance***) **(DA)** – domain of the particles are located (coordinates) in 6D phase space, where their motion in electromagnetic field of the facility is stable under the influence perturbations. Here the perturbations are:

- systematic and random errors of the lattice magnets and RF-stations;
- space charge force;
- impedance of the beam pipe;
- etc.

In this works, only **transvers** DA are considered (without the synchrotron motion).

Let us introduce the concept of the maximal initial amplitude of a particle oscillation:

$$A_{x,y}(s) \Leftrightarrow (x, x', y, y') : \forall N_{turn}, \exists A_{x,y}(s) > A'_{x,y}(s), N_{turn} \in \mathbb{Z}^+$$

$A'_{x,y}(s)$ – the geometrical acceptance of the facility.

The **following tasks** are necessary solved for checking this condition:

- find DA by numerical simulation;

Introduction

Dynamic aperture (or ***acceptance***) **(DA)** – domain of the particles are located (coordinates) in 6D phase space, where their motion in electromagnetic field of the facility is stable under the influence perturbations. Here the perturbations are:

- systematic and random errors of the lattice magnets and RF-stations;
- space charge force;
- impedance of the beam pipe;
- etc.

In this works, only **transvers** DA are considered (without the synchrotron motion).

Let us introduce the concept of the maximal initial amplitude of a particle oscillation:

$$A_{x,y}(s) \Leftrightarrow (x, x', y, y') : \forall N_{turn}, \exists A_{x,y}(s) > A'_{x,y}(s), N_{turn} \in \mathbb{Z}^{+}$$

$A'_{x,y}(s)$ – the geometrical acceptance of the facility.

The **following tasks** are necessary solved for checking this condition:

- find DA by numerical simulation;
- estimate the effect of the different perturbation on the DA value;

Introduction

Dynamic aperture (or ***acceptance***) **(DA)** – domain of the particles are located (coordinates) in 6D phase space, where their motion in electromagnetic field of the facility is stable under the influence perturbations. Here the perturbations are:

- systematic and random errors of the lattice magnets and RF-stations;
- space charge force;
- impedance of the beam pipe;
- etc.

In this works, only **transvers** DA are considered (without the synchrotron motion).

Let us introduce the concept of the maximal initial amplitude of a particle oscillation:

$$A_{x,y}(s) \Leftrightarrow (x, x', y, y') : \forall N_{turn}, \exists A_{x,y}(s) > A'_{x,y}(s), N_{turn} \in \mathbb{Z}^+$$

$A'_{x,y}(s)$ – the geometrical acceptance of the facility.

The **following tasks** are necessary solved for checking this condition:

- find DA by numerical simulation;
- estimate the effect of the different perturbation on the DA value;
- compare this value with the acceptance of the facility (150 and $58\pi \cdot mm \cdot mrad$ for the horizontal and vertical plane, respectively).

The MAD-X software using the PTC (Polymorphic tracking code) symplectic tracking algorithm was used for the DA simulation.

Simulation

Magnetic Measurements

Parameter	Dipole magnet Mean	Dipole magnet SD	Quadrupole magnet Mean	Quadrupole magnet SD
At the injection energy $(3{,}2 MeV/u)$				
α (tilt), $mrad$	$-1{,}3$	$1{,}7$	—	$0{,}1$
$dX = dY, mm$	—	—	—	$0{,}1$
$B_0L\ (B_1L), T \cdot mm$	—	$0{,}19$	—	$0{,}06$
$b_2 \cdot 10^{-4}$	$-0{,}8$	$0{,}6$	$-2{,}1$	$4{,}6$
$a_2 \cdot 10^{-4}$	—	—	$1{,}3$	$4{,}3$
$b_3 \cdot 10^{-4}$	—	—	$7{,}6$	$3{,}1$
$b_5 \cdot 10^{-4}$	—	—	$4{,}9$	$0{,}6$
At the extraction energy $(578 MeV/u)$				
α (tilt), $mrad$	$-1{,}2$	$1{,}6$	—	$0{,}1$
$dX = dY, mm$	—	—	—	$0{,}1$
$B_0L\ (B_1L), T \cdot mm$	—	$2{,}19$	—	$0{,}7$
$b_2 \cdot 10^{-4}$	$8{,}5$	$0{,}7$	$-2{,}0$	$4{,}7$
$a_2 \cdot 10^{-4}$	—	—	$1{,}3$	$4{,}0$
$b_3 \cdot 10^{-4}$	—	—	$7{,}1$	$3{,}1$
$b_5 \cdot 10^{-4}$	—	—	$4{,}2$	$0{,}8$

$$b(a)_n = \frac{1}{n!}\frac{r_{ref}^n}{B_{ref}}\frac{\partial^n B_{y(x)}}{\partial x^n};$$

$$b(a)_n^{int} = \frac{\int_{-\infty}^{\infty} b(a)_n(s)}{L_{eff}},$$

n is the harmonics number (starting from $n = 0$); B_{ref} is the main component of the field at $r_{ref} = 30mm$; L_{eff} is the effective length of the magnet.

Tracking Parameters

The dependence of DA on the number of turns can be estimated as:

$$DA(N_{turn}) = A + \frac{B}{\log_{10}(N_{turn})}; A, B = const.$$

- number of turns for tracking is chosen, on the one hand, providing an acceptable deviation of the DA value from the **asymptotic value (A)**, and, on the other hand, as small as possible to reduce the simulation time;
- to calculate the tune values (see bellow), the nuber of turns has to be proportional to $2^N, N \in \mathbb{Z}^+$;
- To find the parameters A and B and hence, the asymptotic value of the DA, a long-term simulations are performed which is a separete study.

Tracking Parameters

The dependence of DA on the number of turns can be estimated as:

$$DA(N_{turn}) = A + \frac{B}{\log_{10}(N_{turn})}; A, B = const.$$

- number of turns for tracking is chosen, on the one hand, providing an acceptable deviation of the DA value from the **asymptotic value (A)**, and, on the other hand, as small as possible to reduce the simulation time;
- to calculate the tune values (see bellow), the nuber of turns has to be proportional to $2^N, N \in \mathbb{Z}^+$;
- To find the parameters A and B and hence, the asymptotic value of the DA, a long-term simulations are performed which is a separete study.

Calculation for **2D** and **4D** betatron motion **are presented**:

- the particle tracking 2^{10} turns to build-up the phase-plane plot (x, p_x) and (y, p_y) and correspondence the tune vs. initial amplitude $\nu_{x/y} = f(x/y)$ (2D DA);
- the particle tracking 5000 turns to calculate 4D DA $(A_{x,y})$.

Simulation Modes

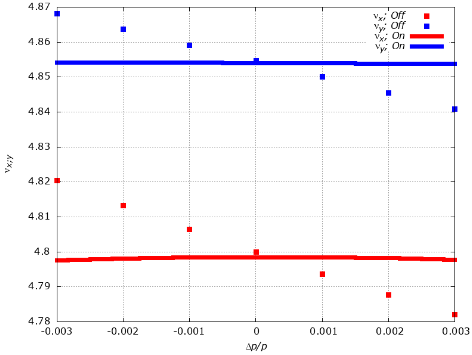

Simulation modes:

- without errors: No Errors;
- misalignment errors (rotation around the longitudinal axis and displacement of the magnetic axis of the element relative to geometric axis): Allign;
- misalignment errors (see above) and deviation of the integral value of the main magnetic field (dipole or quadrupole) component of the lattice elements: Allign+Int;
- only mean values of all error types are included: Total;
- the mean values and SD of all error types are included: Total+Rnd (2000 sampling).

Simulation Modes

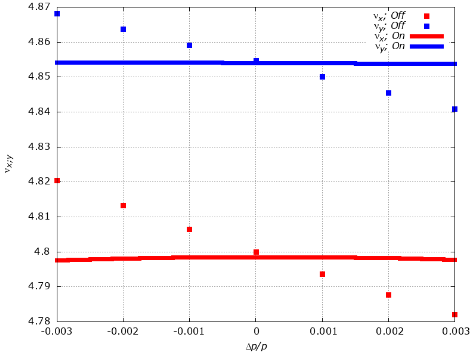

Simulation modes:

- without errors: No Errors;
- misalignment errors (rotation around the longitudinal axis and displacement of the magnetic axis of the element relative to geometric axis): Allign;
- misalignment errors (see above) and deviation of the integral value of the main magnetic field (dipole or quadrupole) component of the lattice elements: Allign+Int;
- only mean values of all error types are included: Total;
- the mean values and SD of all error types are included: Total+Rnd (2000 sampling).

- The harmonics of the magnetic field were determined as absolute thin multipole elements at each of the magnet edges. The harmonics value for each of these elements was defined as half of the integral value.
- The initial tracking point in the center of the straight section of the first superperiod (the injection point into the Booster) were chosen.
- The initial state vector in phase-space was defined as: $\mathrm{s}_0 = (x_0, p_{x0}, y_0, p_{y0})^T$

Results

2D Betatron Motion

The **Poincaré** and **Hénon mapping (sections)** is a common technique for analyzing complex dynamical systems.

- The transformation of coordinates in the phase-space $\mathbf{x}_0 = (x_0, p_{x0}) \mapsto \mathbf{x}_1 = (x_1, p_{x1})$ ($\mathbb{R}^2 \mapsto \mathbb{R}^2$) is described using the **Poincaré map** $(\mathcal{M})$: $\{\mathcal{M}\colon \mathbf{x}_{n+1} = \mathcal{M}^{(1)}(\mathbf{x}_n), \forall n \in \mathbb{Z}^+\}$.
- Introduce the concept of a **one-turn map** to describe the transformation of the phase-space coordinates when passing through all elements of the accelerator: $\mathbf{M} = \mathcal{M}^n \circ \mathcal{M}^{n-1} \circ \cdots \circ \mathcal{M}^2 \circ \mathcal{M}^1$.
- The **Poincaré section** is the set of all of the one-turn maps: $\{\mathbf{M}_1, \mathbf{M}_2, \ldots, \mathbf{M}_n\}$. For a *periodical* lattice structure: $\mathbf{x}(s_0) = \mathbf{x}(s_L) = \mathbf{x}(s_0 + L) \Rightarrow$ for many turns passing through the elements: $\mathbf{x}(s_L) = \mathbf{M}^N(\mathbf{x}(s_0))$.

The **Hénon map (section)** and, also, **action-angle** variables (J, ψ) could be obtained by transformation to the *Normal (Jordan)* form of the *Floquet solution (Floquet transform)*:

$$(\hat{x}, \hat{p}_x) = \mathcal{A}^{-1} \circ (x, p_x),\ \mathcal{A} = \begin{pmatrix} \sqrt{\beta} & 0 \\ -\frac{\alpha}{\sqrt{\beta}} & \frac{1}{\sqrt{\beta}} \end{pmatrix},$$

2D Betatron Motion

The **Poincaré** and **Hénon mapping (sections)** is a common technique for analyzing complex dynamical systems.

- The transformation of coordinates in the phase-space $\mathbf{x}_0 = (x_0, p_{x0}) \mapsto \mathbf{x}_1 = (x_1, p_{x1})$ ($\mathbb{R}^2 \mapsto \mathbb{R}^2$) is described using the **Poincaré map** ($\mathcal{M}$): $\{\mathcal{M} \colon \mathbf{x}_{n+1} = \mathcal{M}^{(1)}(\mathbf{x}_n), \forall n \in \mathbb{Z}^+\}$.
- Introduce the concept of a **one-turn map** to describe the transformation of the phase-space coordinates when passing through all elements of the accelerator: $\mathbf{M} = \mathcal{M}^n \circ \mathcal{M}^{n-1} \circ \cdots \circ \mathcal{M}^2 \circ \mathcal{M}^1$.
- The **Poincaré section** is the set of all of the one-turn maps: $\{\mathbf{M}_1, \mathbf{M}_2, \ldots, \mathbf{M}_n\}$. For a *periodical* lattice structure: $\mathbf{x}(s_0) = \mathbf{x}(s_L) = \mathbf{x}(s_0 + L) \Rightarrow$ for many turns passing through the elements: $\mathbf{x}(s_L) = \mathbf{M}^N(\mathbf{x}(s_0))$.

The **Hénon map (section)** and, also, **action-angle** variables (J, ψ) could be obtained by transformation to the *Normal (Jordan)* form of the *Floquet solution (Floquet transform)*:

$$(\hat{x}, \hat{p}_x) = \mathcal{A}^{-1} \circ (x, p_x),\ \mathcal{A} = \begin{pmatrix} \sqrt{\beta} & 0 \\ -\frac{\alpha}{\sqrt{\beta}} & \frac{1}{\sqrt{\beta}} \end{pmatrix},$$

- the radius of the phase-space trajectory: $R = \sqrt{2J}$;
- one-turn mapping is corresponded to a rotation in the phase-space by an angle $\psi = 2\pi\nu$, ν is the corresponding betatron tune;
- the axis of rotation is an elliptic stable point and the closed phase trajectories are the one-dimensional Kolmogorov–Arnold–Moser (KAM) tori.

2D Betatron Motion

1. Particles tracking with with the corresponding errors of the lattice elements. The initial amplitude of the particles varied $[1; 46]\, mm$ with a step $5\, mm$.
2. Transformation from the Poincaré to section the Hénon section and the action-angle variables.
3. the DA value is defined as the area inside the phase trajectory:

$$A_\psi = \int_0^{2\pi} \int_0^{R(\psi)} dR \cdot d\psi = \frac{1}{2\pi} \int_0^{2\pi} R(\psi)^2 \cdot d\psi \to \lim_{N \to \infty} \frac{1}{N} \sum_{n=1}^{N} [R_n(\psi)]^2 \equiv \langle R(\psi) \rangle \, (\pi \cdot m \cdot rad).$$

2D Betatron Motion

1. Particles tracking with with the corresponding errors of the lattice elements. The initial amplitude of the particles varied $[1; 46]\,mm$ with a step $5\,mm$.
2. Transformation from the Poincaré to section the Hénon section and the action-angle variables.
3. the DA value is defined as the area inside the phase trajectory:

$$A_\psi = \int_0^{2\pi}\int_0^{R(\psi)} dR\cdot d\psi = \frac{1}{2\pi}\int_0^{2\pi} R(\psi)^2\cdot d\psi \to \lim_{N\to\infty}\frac{1}{N}\sum_{n=1}^{N}[R_n(\psi)]^2 \equiv \langle R(\psi)\rangle\,(\pi\cdot m\cdot rad).$$

The 2D DA (A_ψ) calculation results $(\pi\cdot mm\cdot mrad)$

Simulation type	$(\hat{x}, \hat{p}_x)$ Sextupole correctors off	$(\hat{x}, \hat{p}_x)$ Sextupole correctors on	$(\hat{y}, \hat{p}_y)$ Sextupole correctors off	$(\hat{y}, \hat{p}_y)$ Sextupole correctors on
At the injection energy				
No Errors	$400(\infty)$	$400(\infty)$	$400(\infty)$	$400(\infty)$
Total	310	140	340	320
Total+Rnd	310	160	330	260
At the extraction energy				
No Errors	$400(\infty)$	$400(\infty)$	$400(\infty)$	$400(\infty)$
Total	190	220	320	250
Total+Rnd	180	180	310	250

$3{,}2\ MeV/u$

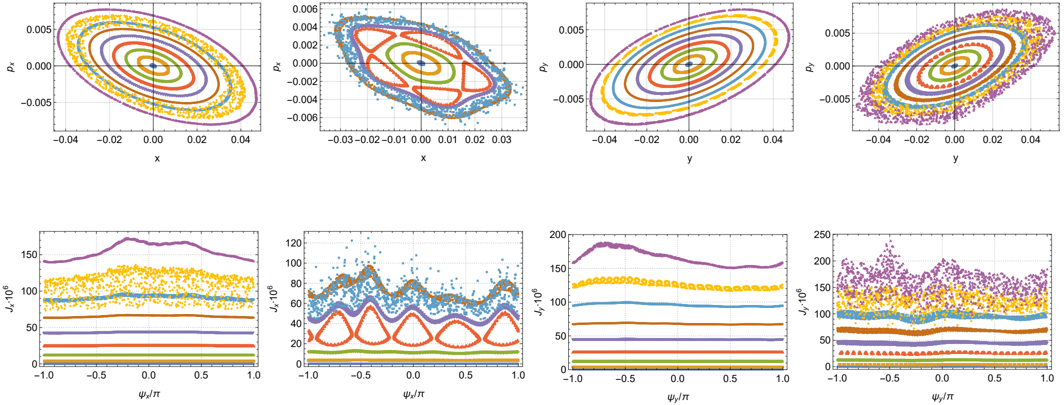

$578\ MeV/u$

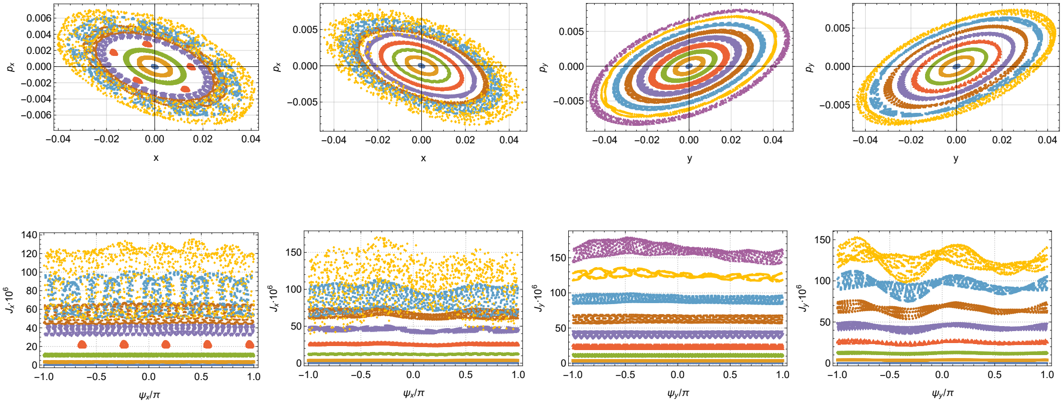

Experemental Results

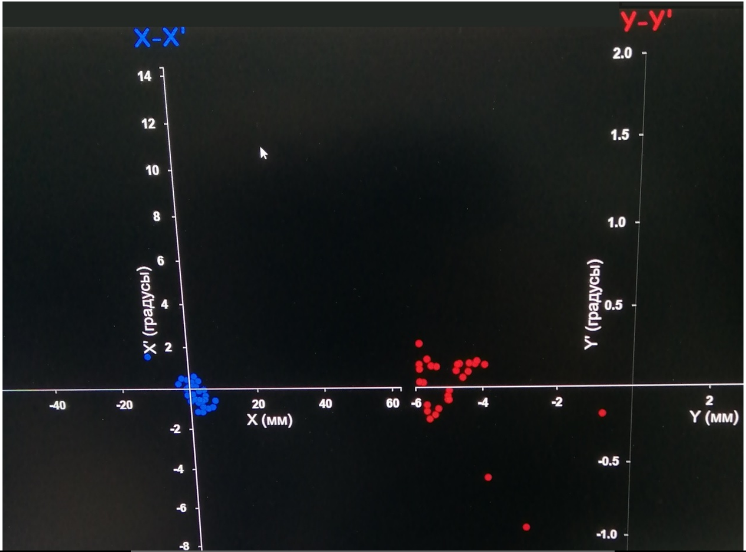

$\nu_{x/y} = f(x/y)$

$3{,}2\,MeV/u$

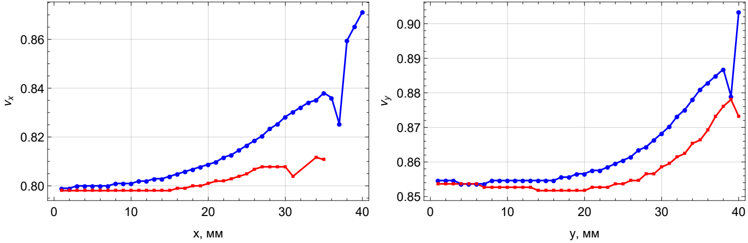

$578\,MeV/u$

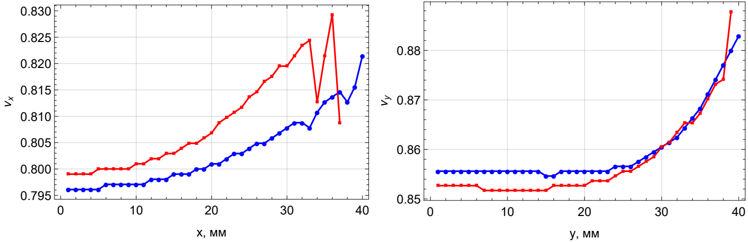

4D Betatron Motion

1. The initial position of the particle was set on the polar grid: $x_0 = r_i \cos\theta_j,\ y_0 = r_i \sin\theta_j,\ 0 \geq \theta_j \geq \pi$.
2. The corresponding beam emittance values: $\varepsilon_x = \frac{x_0^2}{\beta_x},\ \varepsilon_y = \frac{y_0^2}{\beta_y}$.
3. An ensemble of particles with the maximum initial amplitude was selected, when the motion was stable in each azimuth: $r(\theta) \approx r[\theta_j] \longrightarrow \max_i\{r_i(\theta_j, N)\}$.
4. the DA is calculated as

$$A_{r,\theta} = \frac{1}{\pi}\int_0^\pi r(\theta)d\theta \to \lim_{N\to\infty}\frac{1}{N}\sum_{n=1}^{N}[r_n(\theta)]^2 \equiv \langle r(\theta)\rangle\ (m).$$

4D Betatron Motion

1. The initial position of the particle was set on the polar grid: $x_0 = r_i \cos\theta_j,\ y_0 = r_i \sin\theta_j,\ 0 \geq \theta_j \geq \pi$.
2. The corresponding beam emittance values: $\varepsilon_x = \frac{x_0^2}{\beta_x},\ \varepsilon_y = \frac{y_0^2}{\beta_y}$.
3. An ensemble of particles with the maximum initial amplitude was selected, when the motion was stable in each azimuth: $r(\theta) \approx r[\theta_j] \longrightarrow \max_i\{r_i(\theta_j, N)\}$.
4. the DA is calculated as

$$A_{r,\theta} = \frac{1}{\pi}\int_0^{\pi} r(\theta)d\theta \rightarrow \lim_{N\rightarrow\infty}\frac{1}{N}\sum_{n=1}^{N}[r_n(\theta)]^2 \equiv \langle r(\theta)\rangle\ (m).$$

The 4D DA $(A_{r,\theta})$ calculation results (mm)

Simulation type	At the injection energy		At the extraction energy	
	Sextupole correctors off	Sextupole correctors on	Sextupole correctors off	Sextupole correctors on
No Errors	79,0(∞)	63,3	79,0(∞)	63,3
Total	37,4	34,7	38,3	36,3
Total+Rnd	37,2	35,0	38,6	36,6

4D Betatron Motion

$3{,}2\ MeV/u$

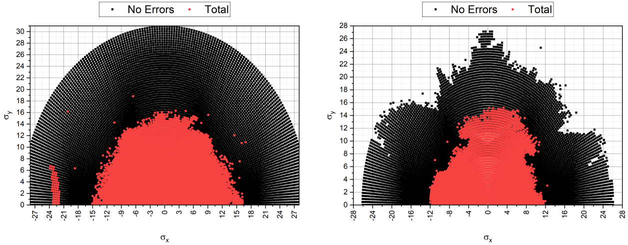

$578\ MeV/u$

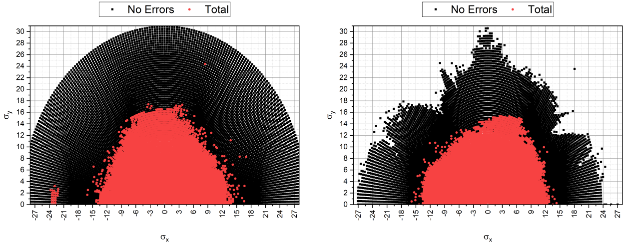

Working Point $\nu_x/\nu_y = 4{,}925/4{,}667$

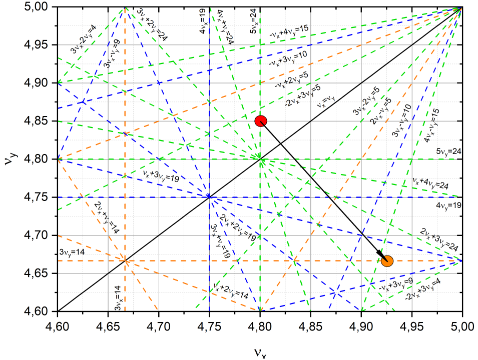

Working Point $\nu_x/\nu_y = 4{,}925/4{,}667$

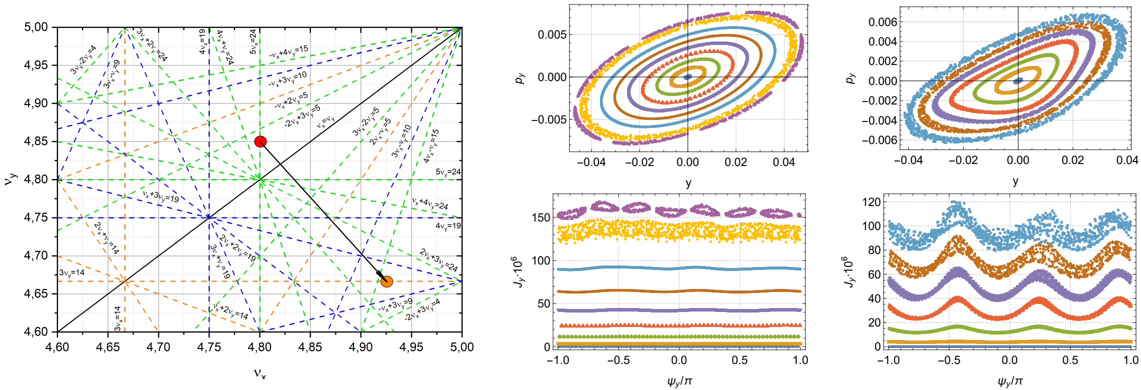

Working Point $\nu_x/\nu_y = 4{,}925/4{,}667$

$3{,}2\ MeV/u$

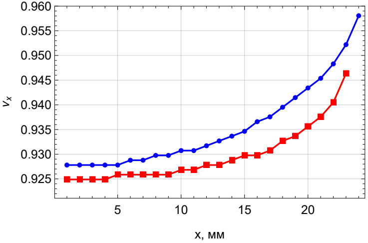

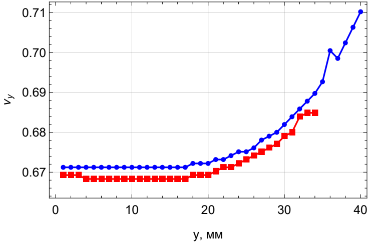

$578\ MeV/u$

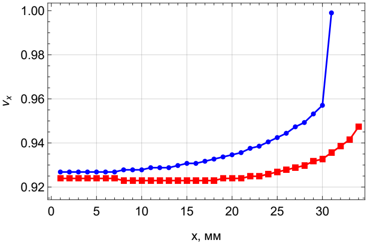

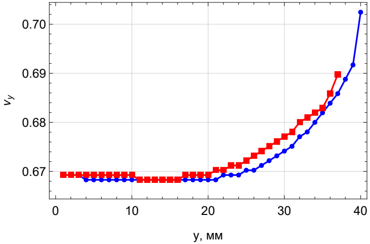

Conclusions

Conclusions

The influence of the errors of the NICA Booster lattice elements on the transverse DA was carried out at the injection and extraction energies. The DA was estimated in 2D and 4D phase space.

- ✓ The Booster lattice model was developed in the MAD-X software. The model allows to take into account the distribution of element parameters based on the results of magnetic measurements and influence of the sextupole correctors.

Conclusions

The influence of the errors of the NICA Booster lattice elements on the transverse DA was carried out at the injection and extraction energies. The DA was estimated in 2D and 4D phase space.

- ✓ The Booster lattice model was developed in the MAD-X software. The model allows to take into account the distribution of element parameters based on the results of magnetic measurements and influence of the sextupole correctors.
- ✓ For the DA simulations and error impact assessment a special technique has been developed. The 2D DA in the horizontal and vertical phase planes exceeds the horizontal and vertical acceptance for all considered simulation modes.

Conclusions

The influence of the errors of the NICA Booster lattice elements on the transverse DA was carried out at the injection and extraction energies. The DA was estimated in 2D and 4D phase space.

- ✓ The Booster lattice model was developed in the MAD-X software. The model allows to take into account the distribution of element parameters based on the results of magnetic measurements and influence of the sextupole correctors.
- ✓ For the DA simulations and error impact assessment a special technique has been developed. The 2D DA in the horizontal and vertical phase planes exceeds the horizontal and vertical acceptance for all considered simulation modes.
- ✓ The numerical analysis of fundamental frequency (NAFF) was used to obtain the tune vs. initial amplitude dependencies $\nu_{x/y} = f(x/y)$ from the tracking results. *Agreement* with the behavior of particles in the corresponding phase space the dependences was obtained (sharp variances shows the presence of regions of stochastic motion and stability islands in the phase portraits).

Conclusions

The influence of the errors of the NICA Booster lattice elements on the transverse DA was carried out at the injection and extraction energies. The DA was estimated in 2D and 4D phase space.

- ✓ The Booster lattice model was developed in the MAD-X software. The model allows to take into account the distribution of element parameters based on the results of magnetic measurements and influence of the sextupole correctors.
- ✓ For the DA simulations and error impact assessment a special technique has been developed. The 2D DA in the horizontal and vertical phase planes exceeds the horizontal and vertical acceptance for all considered simulation modes.
- ✓ The numerical analysis of fundamental frequency (NAFF) was used to obtain the tune vs. initial amplitude dependencies $\nu_{x/y} = f(x/y)$ from the tracking results. *Agreement* with the behavior of particles in the corresponding phase space the dependences was obtained (sharp variances shows the presence of regions of stochastic motion and stability islands in the phase portraits).
- ✓ The 4D DA value 12σ (at the injection and extraction energies) was obtained. A slight decrease of the DA values was observed when the sextupole correctors are switched on (by $\approx 3\sigma$). The maximal initial amplitudes in the $(x, 0)$ and $(0, y)$ directions *correspond* to the 2D DA calculation results

Conclusions

The influence of the errors of the NICA Booster lattice elements on the transverse DA was carried out at the injection and extraction energies. The DA was estimated in 2D and 4D phase space.

- ✓ The Booster lattice model was developed in the MAD-X software. The model allows to take into account the distribution of element parameters based on the results of magnetic measurements and influence of the sextupole correctors.
- ✓ For the DA simulations and error impact assessment a special technique has been developed. The 2D DA in the horizontal and vertical phase planes exceeds the horizontal and vertical acceptance for all considered simulation modes.
- ✓ The numerical analysis of fundamental frequency (NAFF) was used to obtain the tune vs. initial amplitude dependencies $\nu_{x/y} = f(x/y)$ from the tracking results. *Agreement* with the behavior of particles in the corresponding phase space the dependences was obtained (sharp variances shows the presence of regions of stochastic motion and stability islands in the phase portraits).
- ✓ The 4D DA value 12σ (at the injection and extraction energies) was obtained. A slight decrease of the DA values was observed when the sextupole correctors are switched on (by $\approx 3\sigma$). The maximal initial amplitudes in the $(x, 0)$ and $(0, y)$ directions *correspond* to the 2D DA calculation results
- ✓ The working point $\nu_x/\nu_y = 4{,}925/4{,}667$ is located in the vicinity of the 3rd order resonance $3\nu_y = 14$ was considered to test the created Booster lattice model and methodology. The sensitivity of the model to the working point position in the vicinity of vertical and horizontal resonances of different orders and the consistency with the motion of particles in the phase space were obtained in simulation results.

Conclusions

The objects of further research are:

- taking into account the arrangement of the Booster lattice elements;
- simulation at the energy of electron cooling;
- the 6D DA calculation (includes synchrotron motion);
- long-term simulations (to find the asymptotic value of the DA) at three energies (injection, electron cooling, extraction)
- calculation and simulation of the sequential Booster tuning (closed orbit, coupling of the horizontal and vertical motions, natural chromaticity and DA value corrections) and verification the result and the developed technique with the experimental data. **In progress**

Simulation of the dynamic aperture of the NICA booster synchrotron based on magnetic measurement data, *Physics of Particles and Nuclei Letters, 2022, Vol. 19, No. 3, pp. 255–267* were published

Conclusions

The objects of further research are:

- taking into account the arrangement of the Booster lattice elements;
- simulation at the energy of electron cooling;
- the 6D DA calculation (includes synchrotron motion);
- long-term simulations (to find the asymptotic value of the DA) at three energies (injection, electron cooling, extraction)
- calculation and simulation of the sequential Booster tuning (closed orbit, coupling of the horizontal and vertical motions, natural chromaticity and DA value corrections) and verification the result and the developed technique with the experimental data. **In progress**

Simulation of the dynamic aperture of the NICA booster synchrotron based on magnetic measurement data, *Physics of Particles and Nuclei Letters, 2022, Vol. 19, No. 3, pp. 255–267* were published

THANK YOU FOR ATTENTION !!!

Spare Slides

$\nu_{x/y} = f(x/y)$. CO Correction

$3{,}2\, MeV/u$

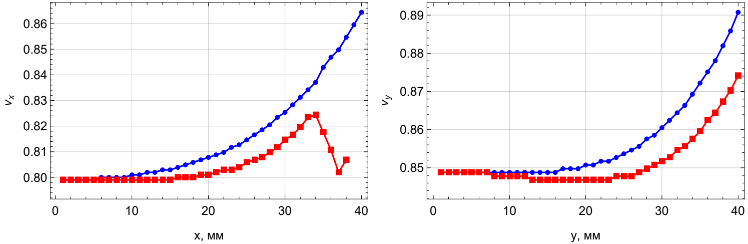

$578\, MeV/u$